Continuous-Flow Reactor Synthesis for Homogeneous 1-nm-Sized Extremely Small High-Entropy Alloy Nanoparticles

Hiroki Minamihara[1], Kohei Kusada[1,2,3]*, Dongshuang Wu[1], Tomokazu Yamamoto[4], Takaaki Toriyama[4], Syo Matsumura[4,5], Loku Singgapulige Rosantha Kumara[6], Koji Ohara[6], Osami Sakata[6], Shogo Kawaguchi[6], Yoshiki Kubota[7], Hiroshi Kitagawa[1]*

[1]Division of Chemistry, Graduate School of Science, Kyoto University, Kitashirakawa-Oiwakecho, Sakyo-ku, Kyoto 606-8502, Japan

[2]The HAKUBI Center for Advanced Research, Kyoto University, Kitashirakawa-Oiwakecho, Sakyo-ku, Kyoto 606-8502, Japan.

[3]JST-PRESTO, Honcho 4-1-8, Kawaguchi, Saitama, 332-0012 Japan.

[4]The Ultramicroscopy Research Center, Kyushu University, 744 Motooka, Nishi-ku, Fukuoka 819-0395, Japan.

[5]Department of Applied Quantum Physics and Nuclear Engineering, Kyushu University, 744 Motooka, Nishi-ku, Fukuoka 819-0395, Japan.

[6]Center for Synchrotron Radiation Research, Japan Synchrotron Radiation Research Institute (JASRI) SPring-8, 1-1-1 Kouto, Sayo-cho, Sayo-gun, Hyogo 679-5198, Japan.

[7]Department of Physical Science, Osaka Prefecture University, 1-1 Gakuen-cho, Naka-ku, Sakai, Osaka 599-8531, Japan.

ABSTRACT: High-entropy alloy nanoparticles (HEA NPs) emerged as catalysts with superior performances that are not shown in monometallic catalysts. Although many kinds of synthesis techniques of HEA NPs have been developed recently, synthesizing HEA NPs with ultrasmall particle size and narrow size distribution remains challenging because most of the reported synthesis methods require high temperatures that accelerate particle growth. This work provides a new methodology for the fabrication of ultrasmall and homogeneous HEA NPs using a continuous-flow reactor with a liquid-phase reduction method. We successfully synthesized ultrasmall IrPdPtRhRu HEA NPs (1.32 ± 0.41 nm), theoretically each consisting of approximately 50 atoms. This average size is the smallest ever reported for HEA NPs. All five elements are homogeneously mixed at the atomic level in each particle. The obtained HEA NPs marked a significantly high hydrogen evolutional reaction (HER) activity with a very small 6-mV overpotential at 10 mA/cm^{-2} in acid, which is one-third of the overpotential of commercial Pt/C. In addition, although mass production of HEA NPs is still difficult, this flow synthesis can provide high productivity with high reproducibility, which is more energy-efficient and suitable for mass production. Therefore, this study reports the 1-nm-sized HEA NPs with remarkably high HER activity and establishes a platform for the production of ultrasmall and homogeneous HEA NPs.

High-entropy alloy nanoparticles (HEA NPs) are of interest in various fields such as energy conversion catalysis.[1–4] The definition of HEA is a solid-solution alloy generally consisting of at least five elements with each elemental ratio between 5 and 35 at.%.[5] Recently, various synthesis techniques of HEA NPs, such as carbothermal shock,[6] fast bed pyrolysis,[7] and solvothermal,[8] have been developed. These methods generally are performed under high temperature to utilize a large configurational entropy in Gibbs free energy ($G = H–TS$). Although these techniques enable the mixing of multi-chemical elements having different properties in nanoparticles, the particle sizes are mostly over 10 nm because high temperature accelerates the atomic diffusion and particle growth. For catalytic application, increasing the surface-to-volume ratio, which often contributes to catalytic activity, is important to efficiently use precious chemical elements. Additionally, some of these techniques require special equipment, creating difficulties for mass production.

Continuous-flow synthesis is an attractive method to efficiently produce many kinds of materials.[9–11] The advantages of this method are precise reaction control and stable reaction condition, which contribute to high selectivity and reproducibility of the products. Recently, this method was applied for mass production of solid-solution alloy NPs by concurrently reducing different metal ions.[12] Given that the particle size can be tuned by the strength of reducing agents in chemical reduction, the combination of a continuous-flow reactor and a strong reducing agent would be one of the best ways for efficiently synthesizing homogeneous ultrasmall HEA NPs.

In this study, we successfully synthesized equimolar extremely small 1.32-nm IrPdPtRhRu HEA NPs by an originally

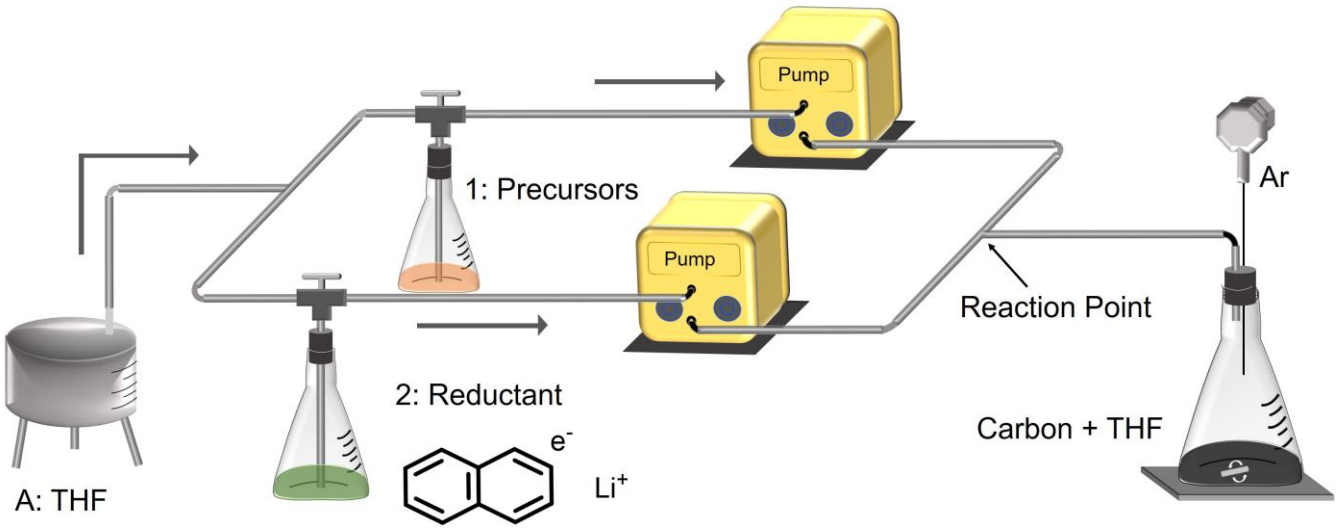

Figure 1. Schematic of the developed continuous-flow reactor.

developed continuous-flow reactor and a strong reducing agent. We investigated the elemental distribution and crystal structure of the obtained NPs by scanning transmission electron microscopy (STEM), energy-dispersive X-ray spectroscopy (EDX), powder X-ray diffraction (PXRD), and pair distribution function (PDF) analyses. The obtained NPs were identified to have the homogeneous distribution of the five elements in ultrasmall NPs with an fcc structure. We further investigated their electrocatalytic activity for hydrogen evolutional reaction (HER). The obtained HEA NPs marked a remarkably small overpotential of 6 mV at 10 mA/cm^{-2} in 1 M $HClO_4$, which is one-third of the overpotential of commercial Pt/C.

Figure 1 shows the developed flow reactor equipped with diaphragm pumps with smooth pulsation for stable supplying solutions and 1/8-inch stainless steel tube (2.2 mm inner diameter) to realize homogeneous mixing precursor and reducing solutions. The connections to the containers of solutions 1 and 2 were three-way cocks sealed by vacuum grease to progress the reaction completely under Ar condition. Solution 1 was a mixture of iridium(III) acetylacetonate, palladium(II) acetylacetonate, platinum(II) acetylacetonate, rhodium(II) acetylacetonate, and ruthenium(III) acetylacetonate dissolved in deoxidized tetrahydro flan (THF). Solution 2 was a strong reducing agent, lithium naphthalenide, easily prepared by mixing Li metal and naphthalene in deoxidized THF and stirring for 1 day in a glove box.[13] Deoxidized THF in A was flowed at a rate of 21.0 mL/min and filled the whole line. Then, solutions 1 and 2 were flowed at 21.0 mL/min and reacted at the mixing point. After only 15 seconds, the black solution was obtained from the exit of the rector and collected in a flask containing carbon support under Ar condition. The obtained NPs with carbon were sonicated for 4 hours and separated and washed by centrifugation. After drying at RT, the obtained NPs were exposed to hydrogen without heating.

The obtained HEA NPs were characterized by high-angle annular dark-field STEM (HAADF-STEM) equipped with EDX. As shown in Figure 2a, a HAADF-STEM image shows that obtained HEA NPs are homogeneously dispersed on carbon. Astonishingly, the average diameter of the NPs is 1.32 ± 0.41 nm, which is remarkably small, consisting of approximately only 50 atoms and more than 70% surface-to-volume ratio, and narrow size distribution (Figure S1). To investigate compositions, we performed EDX mapping and X-ray fluorescence (XRF) analysis. Figure 2b–f shows elemental maps of Ir, Pd, Pt, Rh, and Pd corresponding to the HAADF-STEM image. All five of the elements are homogeneously distributed in the whole area of NPs, suggesting the successful mixing of the elements at the atomic level. Each elemental ratio calculated from these EDX maps is approximately 20%, which is similar to the result given by XRF (Figure S2). The overlay of the elemental maps is shown in Figure S3.

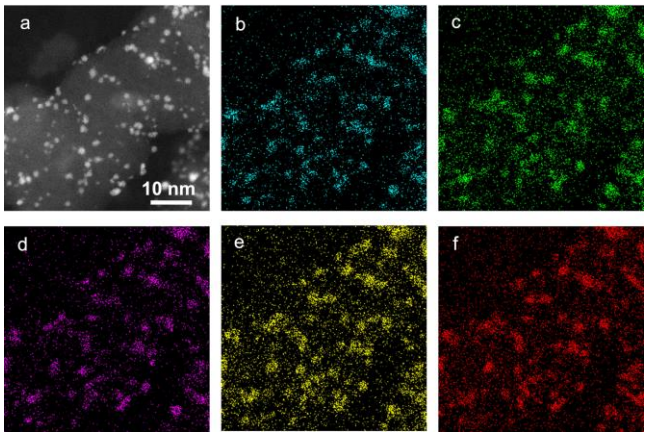

Figure 2. (a) HAADF-STEM image of 1.32 nm HEA NPs. Corresponding EDX maps of (b) Ir-*L*, (c) Pd-*L*, (d) Pt-*L*, (e) Rh-*L*, and (f) Ru-*L*.

To confirm the solid-solution structure, we performed line profile analysis (Figure S4). All five of the elements are uniformly distributed in a small NP. Furthermore, EDX point analysis was conducted to evaluate the homogeneity of composition depending on the particle size from 0.82 to 2.31 nm (Figure S5). The elemental ratio was almost 20% in all the particles. A difference of several percentage points in 0.82 nm is reasonable because this particle ideally consists of only around 13 atoms, and one atom in the particle has a contribution of 8% for elemental ratio. These results strongly support successfully synthesizing very homogeneous ultrasmall HEA NPs.

As shown in Figure 3, the PXRD pattern of 1.32-nm HEA NPs from which carbon and capillary peaks were subtracted (Figure S6) shows very broad peaks originating from ultrasmall

particle size and lattice distortion because of multiple elements with different atomic radii. The XRD pattern was analyzed by Rietveld refinement, and the best fit was obtained by an fcc structure with a lattice constant of 3.8843(8) Å.

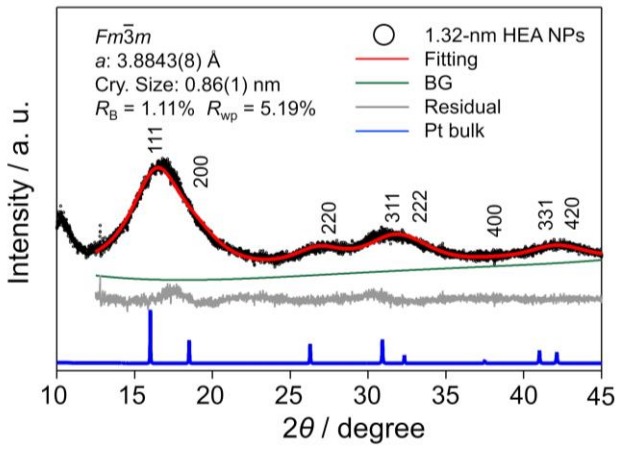

Figure 3. Synchrotron XRD pattern of 1.32-nm HEA NPs and Rietveld refinement results. Experimental data, fitting, background, and residual curves are represented by the black circles and red, green, and gray curves, respectively. Pt bulk data are represented by the blue curve. The X-ray radiation wavelength is 0.630327(7) Å.

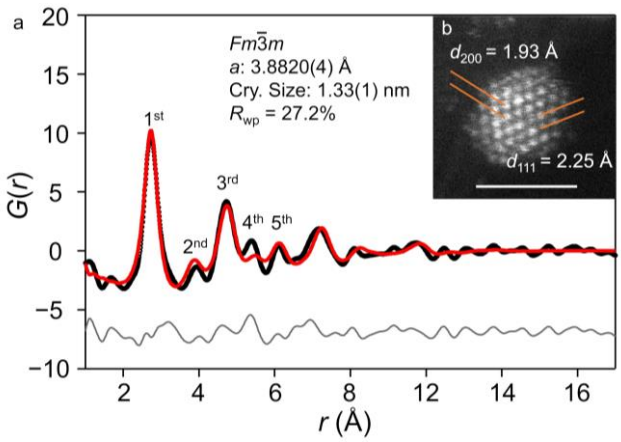

Figure 4. (a) PDF data and the fitting result of 1.32-nm HEA NPs. Experimental data, fitting, and residual curves are represented by the black circles, red and gray curves, respectively. (b) Atomic-resolution HAADF-STEM image of a 1.32-nm HEA NP. The scale bar is 2 nm.

The refined fcc structure was confirmed by a combination of high-energy XRD and PDF analysis (Figure S7). In general, there are two types of scattering from a material; one is Bragg scattering and the other is diffuse scattering. In the case of ultrasmall NPs, the contribution of diffuse scattering becomes prominent.[14,15] Therefore, PDF analysis using both scatterings could be a powerful method to reveal their atomic-scale structures.[16] First, it was found that the PDF peak tops (Figure 4a) were very similar to the atomic distance of the fcc structure obtained from Rietveld refinement (Table S1). Then, we conducted PDF analysis, and the best fit was obtained by an fcc structure with a 3.8820(4) Å lattice parameter and 1.33(1)-nm particle size. In addition, the atomic-resolution HAADF-STEM image of the 1.32-nm HEA NPs in Figure 4b shows 2.25 and 1.94 Å lattice spacing corresponding to the {111} and {200} planes, which are very close to the 2.24 and 1.94 Å calculated from the result of PDF analysis. These results proved that 1.32-nm HEA NPs have an fcc structure.

This ultrasmall size and homogeneous structure in the HEA NPs can be attributed to the combination of a continuous-flow reactor and strong reducing agent. IrPdPtRhRu HEA NPs were previously synthesized by a batch-type chemical reducing method under 503 K for more than 10 min using triethylene glycol as a reducing agent.[1] The temperature and concentration of metal precursors were continually changed because metal precursor solution was added drop by drop into a heated reducing agent. This method provided HEA NPs with a size of 5.5 ± 1.2 nm, with the relatively large particle size and wide size distribution derived from high temperature and inhomogeneous reaction conditions. In this report, we realized lower reaction temperature and homogeneous reaction conditions using a continuous-flow reactor with a strong reducing agent, LiNaph. The E^0 of LiNaph (in THF) is −3.10 V,[17] which is much lower than those of all the precursors. This reducing power can accelerate the concurrent reduction of all the precursors and the nucleation at room temperature, which realizes ultrasmall nanoparticle size and narrow size distribution. Furthermore, this method provides two advantages for catalytic use: LiNaph does not need an additional protecting agent, and high productivity and reproducibility. Generally, very low concentration is needed to synthesize ultrasmall NPs, leading to a lack of productivity, while the continuous-flow method provides high productivity with high reproducibility, which is more energy-efficient and suitable for mass production.[18] In addition, to investigate the effect of the flow rate on particle size, we synthesized HEA NPs with the flow rates of 45 mL/min and 10 mL/min (Figure S8), and confirmed that flow rates did not significantly affect nanoparticle size/distribution in this synthesis.

HER plays an important role in energy conversion for the development of hydrogen-based energy resources. HER catalytic activity of the obtained NPs was investigated to demonstrate the advantage of ultrasmall size in HEA NPs. There was 1 μg of 1.32-nm HEA NPs dropped on a rotating electrode of 3 mm diameter and dried at RT. Commercial Pt/C with 3.42 ± 0.74 nm (Figure S9) and Pt NPs with 1.98 ± 0.80 nm synthesized by the same condition as the HEA NPs (Figure S10) were also prepared as references with 1 μg in metal loaded on electrodes. In Figure 5a, each polarization curve was obtained at a scan rate of 5 mV/s in 1 M $HClO_4$ and normalized by the electrode area (0.0707 cm^{-2}). Interestingly, the activity of 1.32-nm HEA NPs was much higher than that of commercial Pt/C and the synthesized Pt NPs. 1.32-nm HEA NPs marked a significantly small overpotential of 6 mV at 10 mA/cm^{-2}, which is one-third of the overpotential of commercial Pt/C and the synthesized Pt NPs (15.5 mV). This activity is also higher than the synthesized 4.02-nm HEA NPs (9 mV) as shown in Figure S11. Moreover, 1.32-nm HEA NPs achieved a sufficiently high mass activity of 1.6 A/mg at −0.01 V, which is 8.0 times higher than commercial Pt/C. The HEA NPs show one of the best HER activities among reported highly active platinum group metal-based catalysts (Table S2). To investigate the intrinsic activity, turnover frequency (TOF) values of 1.32-nm HEA NPs and the synthesized Pt NPs were calculated by electrochemically active surface area (Figure S12 and S13). At the overpotential of 10 mV, the TOF values of 1.32-nm HEA NPs were 7.5 times higher (4.04 H_2 per second) than that of the synthesized Pt NPs (0.54 H_2 per second).

These results demonstrate that both the size effect and high-entropy effect contributed to the remarkably high intrinsic activity of HEA NPs. It is widely accepted that the intrinsic HER activities such as TOF are mainly explained by the hydrogen adsorption energy which is related to d-band center (ε_d) in the case of monometals and binary alloys.[19] However, for HEA NPs, the surface atoms have wider range distribution of ε_d due to the complex atomic arrangement.[20] The wider range distribution of ε_d of the surface atoms on 1.32-nm HEA NPs may result in the high intrinsic activity which cannot be explained only by hydrogen adsorption energy.

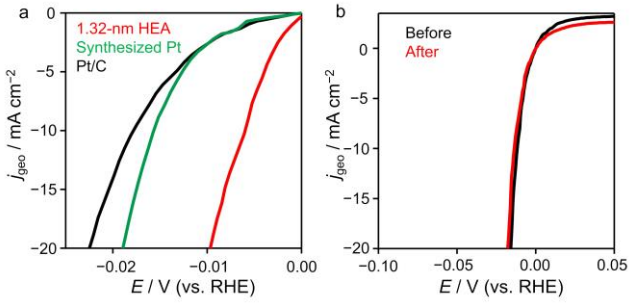

Figure 5. HER performance of 1.32-nm HEA NPs in 1 M $HClO_4$. (a) Polarization curves of 1.32-nm HEA NPs, the synthesized Pt NPs, and commercial Pt/C. (b) Comparison of the polarization curves before and after the durability test.

Especially in acidic conditions, stability is also a very important factor. The polarization curves before and after the durability test (Figure S14) were compared. As shown in Figure 5b, significant degradation was not observed, which indicates the high stability of 1.32-nm HEA NPs. The reason for the high stability of 1.32-nm HEA NPs could be the contribution of a high configurational entropy effect such as sluggish atomic diffusion and solid-solution strengthening.[21]

In summary, we first demonstrated a new methodology in a liquid-phase reduction method for synthesis of homogeneous 1-nm-sized extreme small HEA NPs using a continuous-flow reactor with LiNaph as a strong reducing agent. We successfully synthesized IrPdPtRhRu HEA NPs with 1.32 ± 0.41 nm, the smallest ever reported for HEA NPs. This continuous-flow synthesis method provides the HEA catalyst at least 500 g/day, which is larger than other synthesis methods.[22] In addition, 1.32-nm HEA NPs showed remarkably higher HER activity than commercial Pt/C in acidic conditions. This report will serve as a platform to develop an efficient synthesis method of ultrasmall HEA NPs for practical use.

ASSOCIATED CONTENT

Supporting Information

XRD patterns, STEM-EDX, PDF and electrochemistry data and table. Experimental details and theoretical calculation.

AUTHOR INFORMATION

Corresponding Author

Kohei Kusada: kusada@kuchem.kyoto-u.ac.jp
Hiroshi Kitagawa: kitagawa@kuchem.kyoto-u.ac.jp

Notes

The authors declare no competing financial interests.

ACKNOWLEDGMENT

We acknowledge the support from a Grant-in-Aid for Specially Promoted Research, No. 20H05623 and Grant-in-Aid for Scientific Research (B), No. 21H01762, and JST PRESTO JP20348065. Synchrotron XRD measurements were carried out on beamline BL02B2 at SPring-8 under proposal Nos. 2021A1202 and 2021B1202. The HEXRD were carried out on beamline BL04B2 at SPring-8 under proposal No. 2020A0622. STEM analyses were performed as a part of a program conducted by the Advanced Characterization Nanotechnology Platform sponsored by the Ministry of Education, Culture, Sports, Science and Technology (MEXT) of the Japanese government.

REFERENCES

(1) Wu, D.; Kusada, K.; Yamamoto, T.; Toriyama, T.; Matsumura, S.; Gueye, I.; Seo, O.; Kim, J.; Hiroi, S.; Sakata, O.; Kawaguchi, S.; Kubota, Y.; Kitagawa, H. On the Electronic Structure and Hydrogen Evolution Reaction Activity of Platinum Group Metal-Based High-Entropy-Alloy Nanoparticles. *Chem. Sci.* **2020**, *11* (47), 12731–12736.
(2) Liang, Z.; Song, L.; Deng, S.; Zhu, Y.; Stavitski, E.; Adzic, R. R.; Chen, J.; Wang, J. X. Direct 12-Electron Oxidation of Ethanol on a Ternary Au(Core)-PtIr(Shell) Electrocatalyst. *J. Am. Chem. Soc.* **2019**, *141* (24), 9629–9636.
(3) Amiri, A.; Shahbazian-Yassar, R. Recent Progress of High-Entropy Materials for Energy Storage and Conversion. *J. Mater. Chem. A* **2021**, *9* (2), 782–823.
(4) Kusada, K.; Wu, D.; Kitagawa, H. New Aspects of Platinum Group Metal-Based Solid-Solution Alloy Nanoparticles: Binary to High-Entropy Alloys. *Chem. - A Eur. J.* **2020**, *26* (23), 5105–5130.
(5) Yeh, B. J.-W.; Chen, S.-K.; Lin, S.-J.; Gan, J.-Y.; Chin, T.-G.; Shun, T.-T.; Tsau, C.-H.; Chang, S.-Y. Nanostructured High-Entropy Alloys with Multiple Principal Elements: Novel Alloy Design Concepts and Outcomes. *Adv. Eng. Mater.* **2004**, *6*(5), 299-303.
(6) Yao, Y.; Huang, Z.; Xie, P.; Lacey, S. D.; Jacob, R. J.; Xie, H.; Chen, F.; Nie, A.; Pu, T.; Rehwoldt, M.; Yu, D.; Zachariah, M. R.; Wang, C.; Shahbazian-Yassar, R.; Li, J.; Hu, L. Carbothermal Shock Synthesis of High-Entropy-Alloy Nanoparticles. *Science.* **2018**, *359*(6383), 1489-1494.
(7) Gao, S.; Hao, S.; Huang, Z.; Yuan, Y.; Han, S.; Lei, L.; Zhang, X.; Shahbazian-Yassar, R.; Lu, J. Synthesis of High-Entropy Alloy Nanoparticles on Supports by the Fast Moving Bed Pyrolysis. *Nat. Commun.* **2020**, *11*(1), 2016.
(8) Bondesgaard, M.; Broge, N. L. N.; Mamakhel, A.; Bremholm, M.; Iversen, B. B. General Solvothermal Synthesis Method for Complete Solubility Range Bimetallic and High-Entropy Alloy Nanocatalysts. *Adv. Funct. Mater.* **2019**, *29* (50), 1–9.
(9) Plutschack, M. B.; Pieber, B.; Gilmore, K.; Seeberger, P. H. The Hitchhiker's Guide to Flow Chemistry. *Chem. Rev.* **2017**, *117* (18), 11796–11893.
(10) Britton, J.; Majumdar, S.; Weiss, G. A. Continuous Flow Biocatalysis. *Chem. Soc. Rev.* **2018**, *47* (15), 5891–5918.
(11) Palmacci, E. R.; Plante, O. J.; Hewitt, M. C.; Seeberger, P. H. Automated Synthesis of Oligosaccharides. *Helv. Chim. Acta* **2003**, *86* (12), 3975–3990.
(12) Kusada, K.; Kitagawa, H. Continuous-Flow Syntheses of Alloy Nanoparticles. *Mater. Horizons* **2022**, *9* (2), 547–558.
(13) Schöttle, C.; Bockstaller, P.; Popescu, R.; Gerthsen, D.; Feldmann, C. Sodium-Naphthalenide-Driven Synthesis of Base-Metal Nanoparticles and Follow-up Reactions. *Angew. Chemie - Int. Ed.* **2015**, *54* (34), 9866–9870.
(14) Di Marco, M.; Ballirano, P.; Port, M.; Piscopiello, E.; Couvreur, P.; Dubernet, C.; Sadun, C. Atomic Pair Distribution Function (PDF) Study of Iron Oxide Nanoparticles in Aqueous Suspension. *J. Mater. Chem.* **2009**, *19* (35), 6354–6360.
(15) Harada, M.; Ikegami, R.; Kumara, L. S. R.; Kohara, S.; Sakata, O. Reverse Monte Carlo Modeling for Local Structures of Noble Metal Nanoparticles Using High-Energy XRD and EXAFS. *RSC Adv.* **2019**, *9* (51), 29511–29521.
(16) Kumara, L. S. R.; Sakata, O.; Kohara, S.; Yang, A.; Song, C.; Kusada, K.; Kobayashi, H.; Kitagawa, H. Origin of the Catalytic Activity of Face-Centered-Cubic Ruthenium Nanoparticles

Determined from an Atomic-Scale Structure. *Phys. Chem. Chem. Phys.* **2016**, *18* (44), 30622–30629.
(17) Connelly, N. G.; Geiger, W. E. Chemical Redox Agents for Organometallic Chemistry. *Chem. Rev.* **1996**, *96* (2), 877–910.
(18) Wiles, C.; Watts, P. Continuous Flow Reactors: A Perspective. *Green Chem.* **2012**, *14* (1), 38–54.
(19) Zeradjanin, A. R.; Grote, J. P.; Polymeros, G.; Mayrhofer, K. J. J. A Critical Review on Hydrogen Evolution Electrocatalysis: Re-Exploring the Volcano-Relationship. *Electroanalysis* **2016**, 28 (10), 2256–2269.
(20) Wu, D.; Kusada, K.; Nanba, Y.; Koyama, M.; Yamamoto, T.; Toriyama, T.; Matsumura, S.; Seo, O.; Gueye, I.; Kim, J.; Rosantha Kumara, L. S.; Sakata, O.; Kawaguchi, S.; Kubota, Y.; Kitagawa, H. Noble-Metal High-Entropy-Alloy Nanoparticles: Atomic-Level Insight into the Electronic Structure. *J. Am. Chem. Soc.* **2022**, *144* (8), 3365–3369.
(21) Yeh, J. W. Alloy Design Strategies and Future Trends in High-Entropy Alloys. *Jom* **2013**, *65* (12), 1759–1771.
(22) Xin, Y.; Li, S.; Qian, Y.; Zhu, W.; Yuan, H.; Jiang, P.; Guo, R.; Wang, L. High-Entropy Alloys as a Platform for Catalysis: Progress, Challenges, and Opportunities. *ACS Catal.* **2020**, *10* (19), 11280–11306.

Table of Contents Graphic